

Article

Hierarchical ZSM-5 Zeolite Synthesized Only with Simple Organic Templates

Ying Zhao, Yuanchen Li, Peng Cheng *  and Hongdan Zhang *

Institute of Catalysis for Energy and Environment, College of Chemistry and Chemical Engineering, Shenyang Normal University, Shenyang 110034, China

* Correspondence: chengp1987@126.com (P.C.); zhanghd11@163.com (H.Z.)

Abstract: Hierarchical zeolites have attracted more and more attention due to their excellent diffusion and mass transfer performance. However, synthesis of most hierarchical zeolites requires long-chain organic templates, which could increase preparation cost. Here, hierarchical ZSM-5 zeolites were successfully prepared with simple organic templates (triethylenetetramine) in a rotating oven. Besides hierarchical structure, the crystal size of ZSM-5 also decreased when they were synthesized under dynamic hydrothermal conditions. The samples were analyzed using various physicochemical characterizations, such as X-ray diffraction (XRD), X-ray fluorescence (XRF), scanning electron microscopy (SEM), Fourier transform infrared spectra (FT-IR), temperature-programmed desorption of ammonia (NH₃-TPD) and N₂ adsorption–desorption. The hierarchical ZSM-5 zeolites synthesized in a rotating oven presented better catalytic activity and stability in iso-butane cracking reaction than those synthesized under conventional static hydrothermal conditions.

Keywords: zeolite; hierarchical structure; structure-directing agent; hydrothermal synthesis

1. Introduction

Zeolite is a type of inorganic microporous crystal materials with regular nanopore or cage structures, consisting of TO₄ (T = Si, Al, P, etc.) tetrahedra as the basic structural unit and connected by bridging oxygen atom [1–3]. As one of the most important solid acid catalysts, zeolites are widely used in the field of petrochemical and fine chemical industry due to their unique structures and physicochemical properties [4,5]. However, microporous structure also brings some limitations to zeolites [6]. Firstly, the diffusion and mass transfer of substance are slow. Then, reactants with larger molecular diameters are unable to enter zeolite pores to interact with catalytic active centers. To solve the above issues, a wide variety of approaches have been proposed such as preparation of nanocrystal zeolite materials [7–10], synthesis of extra-large pore zeolite [11–14] and introduction of mesopores or macropores into zeolite to form hierarchical zeolite. Wherein, the synthesis of hierarchical zeolite has become a hot topic due to the advantages of combining microporous zeolite with mesoporous/macroporous materials.

The preparation of hierarchical zeolite could be divided into in situ methods and post-treatment methods. The most common post-treatment method can be achieved by simple dealumination [15–18]/desilication [19–22] of zeolite in acid/alkali solution for the introduction of irregular mesopores or macropores. Hard templating route and soft templating route are the main methods in in situ synthesis. Jacobsen et al. [23] reported the significant results that ZSM-5 nanocrystals with intracrystalline mesopores were successfully prepared with carbon nanoparticles. Zeolite crystals grew around carbon particles and nucleated between them. The pores were large enough, and the gel was concentrated enough to continue to grow in the pore system. Besides carbon nanoparticles, carbon nanotubes or nanofibers [24,25], CaCO₃ nanoparticles [26,27], polymer microspheres [28–31] and biological material [32–35] could be also used to synthesize hierarchical zeolites. The



Citation: Zhao, Y.; Li, Y.; Cheng, P.; Zhang, H. Hierarchical ZSM-5 Zeolite Synthesized Only with Simple Organic Templates. *Inorganics* **2023**, *11*, 297. <https://doi.org/10.3390/inorganics11070297>

Academic Editor: Gary Hix

Received: 4 June 2023

Revised: 30 June 2023

Accepted: 13 July 2023

Published: 14 July 2023



Copyright: © 2023 by the authors. Licensee MDPI, Basel, Switzerland. This article is an open access article distributed under the terms and conditions of the Creative Commons Attribution (CC BY) license (<https://creativecommons.org/licenses/by/4.0/>).

soft template route refers to the synthesis method that the template interacts with silicon or aluminum source in the synthesis system, serving as mesoporous templates. Xiao et al. [36] successfully prepared hierarchical beta zeolite using polydiallyldimethylammonium chloride (PDADMAC) as soft templates due to their high charge density and high dispersion in solution. From the SEM images, it could be observed that there was a partial connection between the hierarchical pores, which may be beneficial for the mass transfer of reactants and products in catalysis. The experimental results showed that the activity of hierarchical zeolites was much higher than that of traditional ZSM-5 catalysts under the same reaction conditions in the catalytic cracking of 1,3,5-triisopropylbenzene. Ryoo et al. [37] firstly synthesized ultra-thin ZSM-5 with long-chain alkyl-quaternary ammonium molecules due to the strong interactions between quaternary ammonium species with the inorganic frameworks. The experimental results indicated that appropriately designed bifunctional surfactants could direct the formation of zeolite structures on the mesoporous and microporous length scales simultaneously and thus yield MFI zeolite nanosheets. And these zeolites dramatically suppressed catalyst deactivation through coke deposition during methanol to gasoline conversion. Recently, Yu et al. [38] reported an anisotropic-kinetics transformation strategy to synthesize single-crystalline hierarchical ZSM-5 zeolites with highly open nanoarchitectures. Due to the improvement of mass transfer efficiency and abundant accessible active site, single crystal ZSM-5 nanocage showed significantly improved catalytic life and lower coking rate in methanol to hydrocarbon reactions. The expensive organic templates also limited the application of hierarchical zeolites to a certain extent.

Herein, we successfully synthesized hierarchical ZSM-5 zeolite with a simple structure-directing agent (triethylenetetramine, denoted as TETA) in a rotating oven. Various methods were used to characterize its physicochemical properties such as X-ray diffraction (XRD), scanning electron microscope (SEM), NH_3 -TPD and N_2 adsorption–desorption. We performed the catalytic cracking of iso-butane on hierarchical ZSM-5, which showed higher catalytic activity compared to ZSM-5 synthesized under conventional hydrothermal condition.

2. Results and Discussion

Figure 1 shows the XRD patterns of solid samples with a TETA/ SiO_2 ratio of 0.3 or 0.4 crystallized for 48 h or 72 h in rotating oven. All spectra showed the characteristic peaks of ZSM-5 at 2θ of 7.9° , 8.9° , 23.1° , 23.9° and 24.3° , which correspond to the standard MFI crystalline structure [39]. These characteristic peaks are associated with [011], [020], [051], [303] and [313] plane. The products with a TETA/ SiO_2 ratio of 0.3 crystallized for 48 h showed pure ZSM-5 zeolite. No obvious diffraction peaks of impurities and amorphous silica were observed in the XRD patterns, and the crystallinity of the sample was relatively high. As the crystallization time increased to 72 h, a characteristic peak at 2θ of 26.7° has appeared, which indicated the sample contained dense phase. Regardless of the crystallization time for 48 h or 72 h, pure ZSM-5 zeolites could not be obtained with a TETA/ SiO_2 ratio of 0.4. However, the crystallization products for 48 h or 72 h were all pure ZSM-5 zeolites under conventional static hydrothermal conditions when the TETA/ SiO_2 ratio was 0.4 (Figure S1). The above results demonstrated that both the content of structure-directing agents and the crystallization time affected the crystallization process significantly under dynamic hydrothermal conditions.

Figure 2 shows the SEM images of solid products under different synthetic conditions. The samples with a TETA/ SiO_2 ratio of 0.3 crystallized in 48 h under conventional static hydrothermal conditions presented typical hexagonal morphology with $20\ \mu\text{m}$ particle size. The crystal surface was smooth and had clear edges and corners (Figure 2a). Meanwhile, the particle size of the products under dynamic hydrothermal conditions reduced to less than $10\ \mu\text{m}$. The prepared particles were uniform polyhedra with smooth surfaces, and the obvious large pores were observed on polyhedron surfaces (Figure 2b). As the crystallization time increased to 72 h, the morphology of samples significantly changed under dynamic hydrothermal conditions, and other phases were produced. The overall morphology was

not very regular, and the crystals have grown to form different morphologies, such as a layered structure on the surface of the grain (Figure 2c). However, the samples with a TETA/SiO₂ ratio of 0.4 crystallized for 48 h under dynamic hydrothermal conditions showed impure ZSM-5 zeolite, covering a large number of spherical crystals (Figure 2d), which was consistent with the XRD results. The crystals had uneven size distribution, and the surface of those was extremely rough.

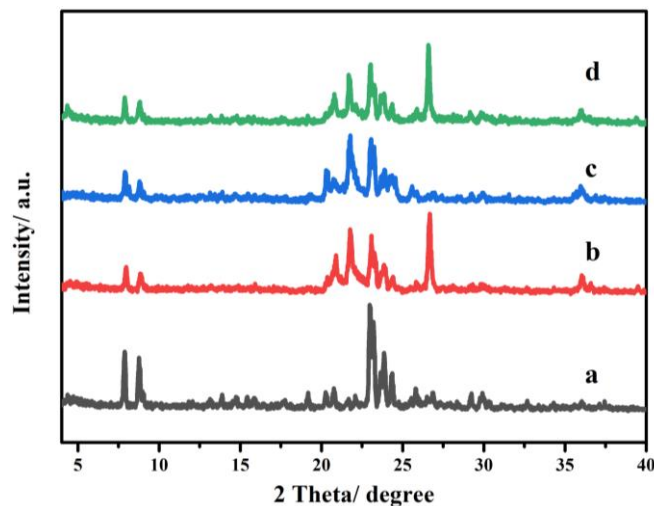


Figure 1. XRD patterns of different samples synthesized: (a) With a TETA/SiO₂ ratio of 0.3 crystallized for 48 h; (b) With a TETA/SiO₂ ratio of 0.3 crystallized for 72 h; (c) With a TETA/SiO₂ ratio of 0.4 crystallized for 48 h; (d) With a TETA/SiO₂ ratio of 0.4 crystallized for 72 h.

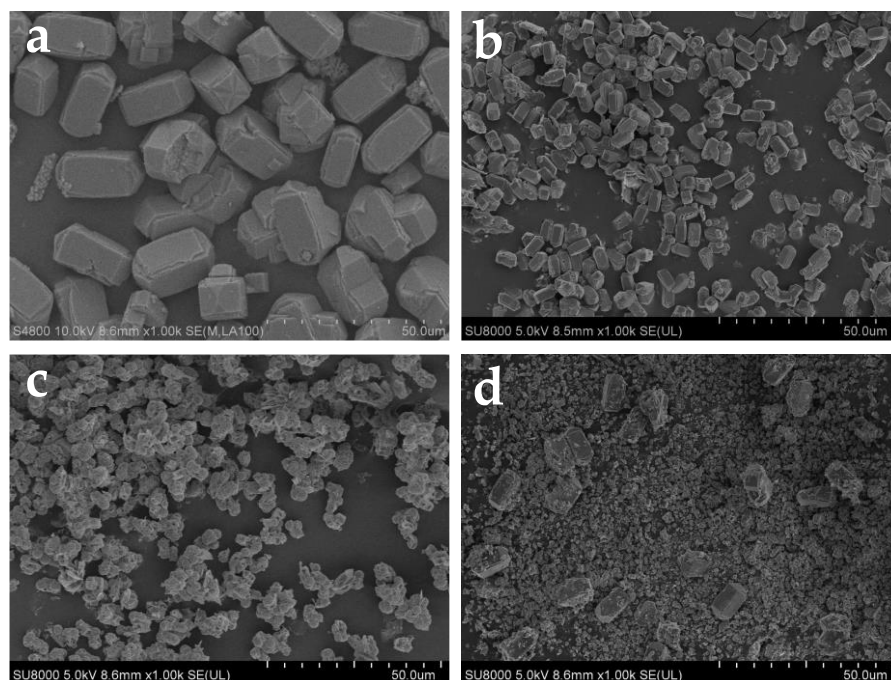


Figure 2. SEM images of samples synthesized under: (a) Conventional static hydrothermal conditions with a TETA/SiO₂ ratio of 0.3 crystallized for 48 h; (b) Dynamic hydrothermal conditions with a TETA/SiO₂ ratio of 0.3 crystallized for 48 h; (c) Dynamic hydrothermal conditions with a TETA/SiO₂ ratio of 0.3 crystallized for 72 h; (d) Dynamic hydrothermal conditions with a TETA/SiO₂ ratio of 0.4 crystallized for 48 h.

Figure S2 shows the N₂ adsorption isotherms of the corresponding products under conventional static/dynamic hydrothermal conditions, and both are typical type-I isotherms.

However, there is an additional closed hysteresis loop (H4) in the range of relative pressure $P/P_0 = 0.4-1.0$ in the N_2 adsorption isotherms of ZSM-5-R, which proves the existence of mesopores. The elemental composition and textual parameters were collected in Table 1. Though the samples were prepared under different hydrothermal conditions, there was no significant difference in SiO_2/Al_2O_3 ratio. The micropore volume of both the products were more than $0.11 \text{ cm}^3 \text{ g}^{-1}$, which demonstrated both the products had good crystallinity. Meanwhile, the sample ZSM-5-R had larger external surface area and mesopore volume than ZSM-5-C. Perez-Ramirez et al. defined the hierarchy factor (HF) as being the product of the relative micropore volume ($V_{\text{micro}}/V_{\text{total}}$) and the relative mesopore surface area ($S_{\text{meso}}/S_{\text{BET}}$) for the first time [40]. The results indicated that ZSM-5-C presented a typical example of pure microporous zeolite, and ZSM-5-R showed zeolites with a small amount of mesoporous systems. The results demonstrated that dynamic hydrothermal conditions were beneficial for synthesizing hierarchical zeolites.

Table 1. The elemental composition and textual parameters of ZSM-5-R and ZSM-5-C.

Sample	SiO_2/Al_2O_3 ³	S_{BET} ($\text{m}^2 \text{ g}^{-1}$)	S_{ext} ($\text{m}^2 \text{ g}^{-1}$)	V_{mic} ($\text{cm}^3 \text{ g}^{-1}$)	V_{meso} ($\text{cm}^3 \text{ g}^{-1}$)	Hierarchy Factor
ZSM-5-R ¹	76.9	314	91	0.12	0.05	0.105
ZSM-5-C ²	77.2	330	86	0.13	0.03	0.075

¹ The solid sample synthesized at 443 K for 48 h with a TETA/ SiO_2 ratio of 0.3 in a rotating oven was denoted as ZSM-5-R. ² The solid sample synthesized at 443 K for 48 h with a TETA/ SiO_2 ratio of 0.3 in a conventional oven was denoted as ZSM-5-C. ³ The SiO_2/Al_2O_3 ratio was determined using XRF.

ATR method was used to test FTIR spectra. Spectral correction was performed by recording the background spectrum of the sample chamber before sample measurement. The single channel background spectrum was recorded first, and then the single channel sample spectrum was collected. And the effect of water and carbon dioxide in the air was removed by compensating for the atmosphere. The FTIR spectra of ZSM-5-R and ZSM-5-C are shown in Figure 3. Five IR characteristic absorption peaks of both solid samples were detected at 438, 540, 790, 1068 and 1220 cm^{-1} , which indicated that there were no differences in structure between ZSM-5-R and ZSM-5-C. The obvious band at 540 cm^{-1} is ascribed to a double five-membered rings vibration peak of pentasil zeolite [41–43]. The intensity of band at 540 cm^{-1} could be used to determine the crystallinity of the ZSM-5 zeolites [44]. The bands at 1220 and 1068 cm^{-1} are assigned to the asymmetric stretching vibration peak of the external and internal T–O tetrahedron, respectively [45]. The band at 438 cm^{-1} is attributed to the bending vibration peak of the Si–O chemical bond [46]. The band at 790 cm^{-1} is assigned to the symmetric stretching vibrations of the internal tetrahedron structure of ZSM-5 zeolite [47].

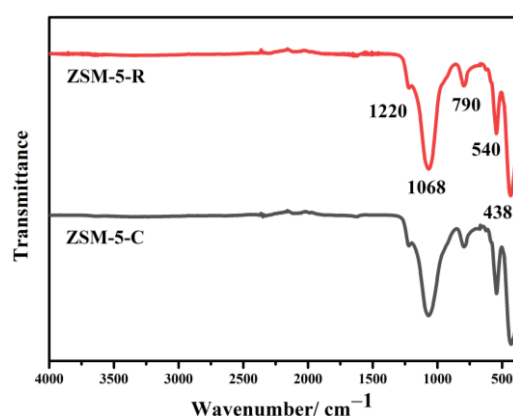


Figure 3. FTIR spectra of different samples.

The acidity of ZSM-5-R and ZSM-5-C samples was analyzed using NH_3 -TPD (Figure 4), which was an important factor affecting the catalytic activity of zeolite. Two obvious NH_3 desorption peaks of both products were observed in the range of 100–250 °C and 300–450 °C, which are corresponding to weak acid sites and strong acid sites, respectively. And the NH_3 desorption peak areas correspond to the amount of acid sites. It could be seen that there was no significant shift for the desorption peak and no significant change for peak area of both solid samples due to the similar $\text{SiO}_2/\text{Al}_2\text{O}_3$ ratio.

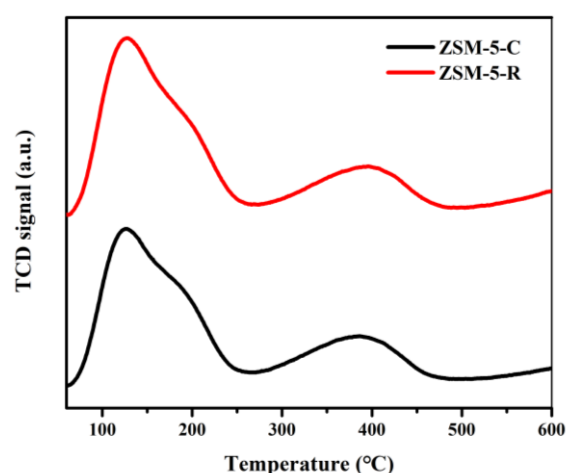


Figure 4. NH_3 -TPD profiles of ZSM-5-R and ZSM-5-C.

The catalytic cracking experiments of iso-butane were performed on ZSM-5-R and ZSM-5-C. We investigated the catalytic activity and stability of the two catalysts during 800 min on stream at 625 °C. At first, the conversion of iso-butane on both catalysts was roughly the same (around 90%). After running for 800 min, the conversion of iso-butane on ZSM-5-R decreased to nearly 50%, still 20% higher than that on ZSM-5-C (Figure 5a). Figure 5b shows the selectivity of ethylene and propylene on the above catalysts. The selectivity of ethylene and propylene on ZSM-5-C consistently decreased. However, that on ZSM-5-R showed a trend of first decreasing and then increasing. After 800 min of reaction, the selectivity of ethylene and propylene on ZSM-5-R was 13% higher than that on ZSM-5-C. ZSM-5-R exhibited higher catalytic activity due to the hierarchical structure.

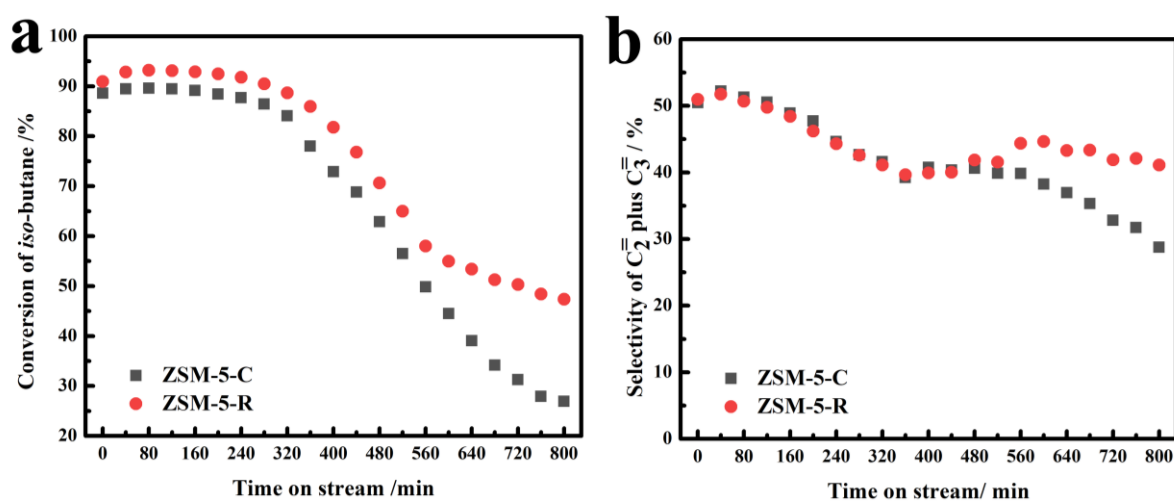


Figure 5. (a) The conversion of iso-butane and (b) the yield of ethylene and propylene on ZSM-5-R and ZSM-5-C as a function of time on stream for 800 min test at 625 °C.

3. Materials and Methods

3.1. Materials

The chemicals used in this study were colloidal silica (LUDOX HS-40), sodium hydroxide (AR, 96%, Sinopharm Chemical Reagent Co., Ltd., Shanghai, China), sodium aluminate (AR, NaAlO₂, Al₂O₃ > 41 wt %, Shanghai Sinopharm Chemical Reagent Co., Ltd., Shanghai, China), triethylenetetramine (AR, 98%, Dongxing Chemical Reagent Co., Ltd., Shenyang, China), ammonium chloride (AR, 97%, Damao Chemical Reagent Co., Ltd., Tianjin, China) and ultrapure deionized water (18.2 MΩ·cm). All reagents were used without any further purification.

3.2. Synthesis of ZSM-5/Hierarchical ZSM-5

ZSM-5 and hierarchical ZSM-5 zeolites were synthesized from the initial aluminosilicate gels with molar composition of SiO₂: 0.013 Al₂O₃: 0.037 Na₂O: 14.60 H₂O: (0.2–0.4) TETA. Typically, 0.17 g of NaAlO₂ was dissolved in 14.17 g of H₂O stirring until the solution became clear. Then, 0.16 g of NaOH was added into the solution, followed by the addition of 2.40/3.60/4.80 g of TETA stirring for 10 min. Finally, 12.30 g of colloidal silica was added to the mixtures dropwise with stirring for 12 h. The final mixtures were transferred into a 100 mL autoclave and heated at 443 K for 48 h or 72 h in a conventional oven or a rotating oven at 25 rpm. The solid products were collected by filtration, washed thoroughly with deionized water until the filtrate was neutral, and dried in air at 333 K overnight. The obtained products were calcined at 823 K for 5 h to remove the organic templates. Subsequently, they were fully stirred for 4 h in a 10% ammonium chloride solution at 353 K twice. The exchanged samples were calcined at 823 K for 5 h.

3.3. Characterizations

The X-ray diffraction (XRD) patterns were recorded on a Rigaku Ultima IV diffractometer equipped with Cu K α radiation ($\lambda = 1.5418 \text{ \AA}$) and operated at 40 kV and 30 mA in the range of 2θ value between 4° and 40° at a scan rate of 6° min⁻¹. Nitrogen adsorption/desorption measurements were carried out on a Micromeritics 2020 analyzer at 77.35 K after the products were degassed at 623 K under vacuum. The quartz tube containing samples should be weighed accurately before and after degassing treatment. And the quartz tube was installed on the physical adsorption device, adding sufficient liquid nitrogen into the Dewar bottle, and then the characterization could be started. The elemental composition of ZSM-5/hierarchical ZSM-5 samples was measured using X-ray fluorescence (XRF) on a Thermo Scientific ARL PERFORM'X spectrometer, Dreieich, Germany. The morphology of crystals was confirmed using scanning electron microscopy (SEM, Hitachi, S4800, Tokyo, Japan). The prepared samples were sprayed with gold to increase their conductivity for testing. Fourier transform infrared spectra (FT-IR) of the samples were recorded utilizing a Bruker Tensor II spectrophotometer, Leipzig, Germany. Scanning of room environment was carried out as the experimental background at ambient temperature. The influence of water and carbon dioxide in the air was removed through atmosphere compensation in advanced settings. Subsequently, the powder samples were placed on the ATR sample stage and were tested with a scanning range of 400–4000 cm⁻¹ and scanning time of 32 s. The acid site density of the synthesized materials was determined using temperature-programmed desorption of ammonia (NH₃-TPD, Micromeritics AutoChem 2920 II, Norcross, GA, USA). Under the condition of argon gas at 300 °C and 40 mL/min, pre-treatment was carried out for 30 min, followed by cooling down to 60 °C. 5% of NH₃/He mixture was introduced into the reaction sample tube for purging with a flow rate of 40 mL/min, and the purging was carried out for 20 min to allow the ZSM-5 zeolites to adsorb NH₃ absolutely. Then, pure argon with a flow rate of 40 mL/min was introduced into the reaction sample tube to purge the NH₃ adsorbed on the surface of the samples. After the baseline stabilized, the temperature started rising to 710 °C at 10 °C/min, and the TCD signal of NH₃ desorption was recorded between 100 and 710 °C.

3.4. Catalytic Reaction

The catalytic cracking experiments of iso-butane were performed on a continuous fixed-bed flow reactor at atmospheric pressure. The protective gas N₂ was firstly introduced into the chromatography, and then the fully automatic air source, hydrogen generator and gas chromatography were turned on. Then, a suitable operating method was chosen. When the detector temperature reached 150 °C, the test could be started until the baseline gradually stabilized. Typically, 0.3 g (40–60 mesh) of catalysts was filled in the middle of the quartz tube, which were heated to 625 °C for 30 min in N₂ flow. Then, the iso-butane (volume fraction was 5%) was also passed through the reactor. The reaction products were analyzed on-line by a gas chromatograph (GC9790 II) equipped with a capillary column (30 m, inner diameter 530 μm) and FID detector. The calculation formulae for C₄ alkane cracking data are as follows:

$$\text{C4H10 Conversion\%} = \frac{c(\text{C4H10, in}) - c(\text{C4H10, out})}{c(\text{C4H10, in})}$$

$$\text{CmHn Selectivity\%} = \frac{c(\text{CmHn} \times \frac{n}{4})}{c(\text{C4H10, in}) - c(\text{C4H10, out})}$$

$$\text{CmHn Yield\%} = \text{C4H10 Conversion} \times \text{CmHn Selectivity}$$

4. Conclusions

In summary, we have developed an effective, inexpensive and simple strategy for synthesizing hierarchical ZSM-5 zeolites without any complex long-chain organic templating agents. Hierarchical ZSM-5 zeolite was successfully prepared only with simple organic templates (triethylenetetramine) in a rotating oven. Compared with conventional static hydrothermal synthesis, ZSM-5 zeolite synthesized in a rotating oven had smaller particle size and hierarchical structure. SEM images and N₂ adsorption–desorption confirmed macropores/mesopores in ZSM-5-R zeolite. There was no difference for the elemental composition, structure and acidity between ZSM-5-R and ZSM-5-C. In the catalytic cracking reaction of iso-butane, the conversion of iso-butane and the selectivity of ethylene and propylene were higher after running for 300 min on ZSM-5-R zeolite due to its hierarchical structure. It provided a new route for synthesis of hierarchical zeolite with simple structure-directing agents.

Supplementary Materials: The following supporting information can be downloaded at: <https://www.mdpi.com/article/10.3390/inorganics11070297/s1>, Figure S1: XRD patterns of different samples synthesized under conventional static hydrothermal conditions; Figure S2: N₂ adsorption isotherms of ZSM-5-R and ZSM-5-C.

Author Contributions: Conceptualization, P.C. and H.Z.; methodology, P.C.; analysis, Y.Z., P.C. and H.Z.; investigation, Y.Z. and Y.L.; data curation, Y.Z. and Y.L.; writing—original draft preparation, H.Z.; writing—review and editing, P.C. and H.Z.; funding acquisition, P.C. and H.Z. All authors have read and agreed to the published version of the manuscript.

Funding: This research was funded by the National Natural Science Foundation of China (Grant No. 22202137 and 22172102), LiaoNing Revitalization Talents Program (XLYC2007190), Shenyang Young and Middle-aged Scientific and Technological Innovation Talents Support Plan (RC210044).

Data Availability Statement: The data presented in this study are available on request from the corresponding author.

Conflicts of Interest: The authors declare no conflict of interest.

References

1. Chen, L.-H.; Sun, M.-H.; Wang, Z.; Yang, W.; Xie, Z.; Su, B.-L. Hierarchically Structured Zeolites: From Design to Application. *Chem. Rev.* **2020**, *120*, 11194–11294. [[CrossRef](#)] [[PubMed](#)]
2. Shamzhy, M.; Opanasenko, M.; Concepción, P.; Martínez, A. New trends in tailoring active sites in zeolite-based catalysts. *Chem. Soc. Rev.* **2019**, *48*, 1095–1149. [[CrossRef](#)] [[PubMed](#)]
3. Li, K.; Valla, J.; Garcia-Martinez, J. Realizing the Commercial Potential of Hierarchical Zeolites: New Opportunities in Catalytic Cracking. *ChemCatChem* **2014**, *6*, 46–66. [[CrossRef](#)]
4. Li, Y.; Yu, J. New Stories of Zeolite Structures: Their Descriptions, Determinations, Predictions, and Evaluations. *Chem. Rev.* **2014**, *114*, 7268–7316. [[CrossRef](#)] [[PubMed](#)]
5. Davis, M.E. Ordered porous materials for emerging applications. *Nature* **2002**, *417*, 813–821. [[CrossRef](#)]
6. Tao, Y.; Kanoh, H.; Abrams, L.; Kaneko, K. Mesopore-Modified Zeolites: Preparation, Characterization, and Applications. *Chem. Rev.* **2006**, *106*, 896–910. [[CrossRef](#)]
7. Peng, C.; Liu, Z.; Horimoto, A.; Anand, C.; Yamada, H.; Ohara, K.; Sukenaga, S.; Ando, M.; Shibata, H.; Takewaki, T.; et al. Preparation of nanosized SSZ-13 zeolite with enhanced hydrothermal stability by a two-stage synthetic method. *Microporous Mesoporous Mater.* **2018**, *255*, 192–199. [[CrossRef](#)]
8. Zhang, X.; Liu, D.; Xu, D.; Asahina, S.; Cychosz, K.A.; Agrawal, K.V.; Al Wahedi, Y.; Bhan, A.; Al Hashimi, S.; Terasaki, O.; et al. Synthesis of Self-Pillared Zeolite Nanosheets by Repetitive Branching. *Science* **2012**, *336*, 1684–1687. [[CrossRef](#)]
9. Ramos, F.S.O.; Pietre, M.K.D.; Pastore, H.O. Lamellar zeolites: An oxymoron? *RSC Adv.* **2013**, *3*, 2084–2111. [[CrossRef](#)]
10. Corma, A.; Fornés, V.; Díaz, U. ITQ-18 a new delaminated stable zeolite. *Chem. Commun.* **2001**, *24*, 2642–2643. [[CrossRef](#)]
11. Li, J.; Gao, Z.R.; Lin, Q.-F.; Liu, C.; Gao, F.; Lin, C.; Zhang, S.; Deng, H.; Mayoral, A.; Fan, W.; et al. A 3D extra-large-pore zeolite enabled by 1D-to-3D topotactic condensation of a chain silicate. *Science* **2023**, *379*, 283–287. [[CrossRef](#)]
12. Corma, A.; Díaz-Cabañas, M.J.; Jordá, J.L.; Martínez, C.; Moliner, M. High-throughput synthesis and catalytic properties of a molecular sieve with 18- and 10-member rings. *Nature* **2006**, *443*, 842–845. [[CrossRef](#)]
13. Jiang, J.; Yu, J.; Corma, A. Extra-Large-Pore Zeolites: Bridging the Gap between Micro and Mesoporous Structures. *Angew. Chem. Int. Ed.* **2010**, *49*, 3120–3145. [[CrossRef](#)]
14. Kang, J.H.; Xie, D.; Zones, S.I.; Smeets, S.; McCusker, L.B.; Davis, M.E. Synthesis and Characterization of CIT-13, a Germanosilicate Molecular Sieve with Extra-Large Pore Openings. *Chem. Mater.* **2016**, *28*, 6250–6259. [[CrossRef](#)]
15. Ren, S.; Liu, G.; Wu, X.; Chen, X.; Wu, M.; Zeng, G.; Liu, Z.; Sun, Y. Enhanced MTO performance over acid treated hierarchical SAPO-34. *Chin. J. Catal.* **2017**, *38*, 123–130. [[CrossRef](#)]
16. González, M.D.; Cesteros, Y.; Salagre, P. Comparison of dealumination of zeolites beta, mordenite and ZSM-5 by treatment with acid under microwave irradiation. *Microporous Mesoporous Mater.* **2011**, *144*, 162–170. [[CrossRef](#)]
17. Hua, Z.L.; Zhou, J.; Shi, J.L. Recent advances in hierarchically structured zeolites: Synthesis and material performances. *Chem. Commun.* **2011**, *47*, 10536–10547. [[CrossRef](#)]
18. Giudici, R.; Kouwenhoven, H.W.; Prins, R. Comparison of nitric and oxalic acid in the dealumination of mordenite. *Appl. Catal. A: Gen.* **2000**, *203*, 101–110. [[CrossRef](#)]
19. Verboekend, D.; Pérez-Ramírez, J. Design of hierarchical zeolite catalysts by desilication. *Catal. Sci. Technol.* **2011**, *1*, 879–890. [[CrossRef](#)]
20. Sommer, L.; Mores, D.; Svelle, S.; Stöcker, M.; Weckhuysen, B.M.; Olsbye, U. Mesopore formation in zeolite H-SSZ-13 by desilication with NaOH. *Microporous Mesoporous Mater.* **2010**, *132*, 384–394. [[CrossRef](#)]
21. Svelle, S.; Sommer, L.; Barbera, K.; Vennestrøm, P.N.R.; Olsbye, U.; Lillerud, K.P.; Bordiga, S.; Pan, Y.-H.; Beato, P. How defects and crystal morphology control the effects of desilication. *Catal. Today* **2011**, *168*, 38–47. [[CrossRef](#)]
22. Bonilla, A.; Baudouin, D.; Pérez-Ramírez, J. Desilication of ferrierite zeolite for porosity generation and improved effectiveness in polyethylene pyrolysis. *J. Catal.* **2009**, *265*, 170–180. [[CrossRef](#)]
23. Jacobsen, C.J.H.; Madsen, C.; Houzvicka, J.; Schmidt, I.; Carlsson, A. Mesoporous Zeolite Single Crystals. *J. Am. Chem. Soc.* **2000**, *122*, 7116–7117. [[CrossRef](#)]
24. Schmidt, I.; Boisen, A.; Gustavsson, E.; Ståhl, K.; Pehrson, S.; Dahl, S.; Carlsson, A.; Jacobsen, C.J.H. Carbon Nanotube Templated Growth of Mesoporous Zeolite Single Crystals. *Chem. Mater.* **2001**, *13*, 4416–4418. [[CrossRef](#)]
25. Janssen, A.H.; Schmidt, I.; Jacobsen, C.J.H.; Koster, A.J.; de Jong, K.P. Exploratory study of mesopore templating with carbon during zeolite synthesis. *Microporous Mesoporous Mater.* **2003**, *65*, 59–75. [[CrossRef](#)]
26. Zhu, H.; Liu, Z.; Wang, Y.; Kong, D.; Yuan, X.; Xie, Z. Nanosized CaCO₃ as Hard Template for Creation of Intracrystal Pores within Silicalite-1 Crystal. *Chem. Mater.* **2008**, *20*, 1134–1139. [[CrossRef](#)]
27. Ren, L.; Wu, Q.; Yang, C.; Zhu, L.; Li, C.; Zhang, P.; Zhang, H.; Meng, X.; Xiao, F.-S. Solvent-Free Synthesis of Zeolites from Solid Raw Materials. *J. Am. Chem. Soc.* **2012**, *134*, 15173–15176. [[CrossRef](#)]
28. Valtchev, V.; Mintova, S. Layer-by-layer preparation of zeolite coatings of nanosized crystals. *Microporous Mesoporous Mater.* **2001**, *43*, 41–49. [[CrossRef](#)]
29. Huang, L.; Wang, Z.; Sun, J.; Miao, L.; Li, Q.; Yan, Y.; Zhao, D. Fabrication of Ordered Porous Structures by Self-Assembly of Zeolite Nanocrystals. *J. Am. Chem. Soc.* **2000**, *122*, 3530–3531. [[CrossRef](#)]
30. Zhu, G.; Qiu, S.; Gao, F.; Li, D.; Li, Y.; Wang, R.; Gao, B.; Li, B.; Guo, Y.; Xu, R.; et al. Template-assisted self-assembly of macro-micro bifunctional porous materials. *J. Mater. Chem.* **2001**, *11*, 1687–1693. [[CrossRef](#)]

31. Wang, X.D.; Yang, W.L.; Tang, Y.; Wang, Y.J.; Fu, S.K.; Gao, Z. Fabrication of hollow zeolite spheres. *Chem. Commun.* **2000**, *21*, 2161–2162. [[CrossRef](#)]
32. Anderson, M.W.; Holmes, S.M.; Hanif, N.; Cundy, C.S. Hierarchical Pore Structures through Diatom Zeolitization. *Angew. Chem. Int. Ed.* **2000**, *39*, 2707–2710. [[CrossRef](#)]
33. Ocampo, F.; Cunha, J.A.; de Lima Santos, M.R.; Tessonier, J.P.; Pereira, M.M.; Louis, B. Synthesis of zeolite crystals with unusual morphology: Application in acid catalysis. *Appl. Catal. A: Gen.* **2010**, *390*, 102–109. [[CrossRef](#)]
34. Valtchev, V.P.; Smaïhi, M.; Faust, A.-C.; Vidal, L. Equisetum arvense Templating of Zeolite Beta Macrostructures with Hierarchical Porosity. *Chem. Mater.* **2004**, *16*, 1350–1355. [[CrossRef](#)]
35. Dong, A.; Wang, Y.; Tang, Y.; Ren, N.; Zhang, Y.; Yue, Y.; Gao, Z. Zeolitic Tissue Through Wood Cell Templating. *Adv. Mater.* **2002**, *14*, 926–929. [[CrossRef](#)]
36. Xiao, F.-S.; Wang, L.; Yin, C.; Lin, K.; Di, Y.; Li, J.; Xu, R.; Su, D.S.; Schlögl, R.; Yokoi, T.; et al. Catalytic Properties of Hierarchical Mesoporous Zeolites Templated with a Mixture of Small Organic Ammonium Salts and Mesoscale Cationic Polymers. *Angew. Chem. Int. Ed.* **2006**, *45*, 3090–3093. [[CrossRef](#)]
37. Choi, M.; Na, K.; Kim, J.; Sakamoto, Y.; Terasaki, O.; Ryoo, R. Stable single-unit-cell nanosheets of zeolite MFI as active and long-lived catalysts. *Nature* **2009**, *461*, 246–249. [[CrossRef](#)]
38. Chen, G.; Li, J.; Wang, S.; Han, J.; Wang, X.; She, P.; Fan, W.; Guan, B.; Tian, P.; Yu, J. Construction of Single-Crystalline Hierarchical ZSM-5 with Open Nanoarchitectures via Anisotropic-Kinetics Transformation for the Methanol-to-Hydrocarbons Reaction. *Angew. Chem. Int. Ed.* **2022**, *61*, e202200677.
39. Wu, E.L.; Lawton, S.L.; Olson, D.H.; Rohrman, A.C.; Kokotailo, G.T. ZSM-5-type materials. Factors affecting crystal symmetry. *J. Phys. Chem.* **1979**, *83*, 2777–2781. [[CrossRef](#)]
40. Perez-Ramirez, J.; Verboekend, D.; Bonilla, A.; and Abella, S. Zeolite Catalysts with Tunable Hierarchy Factor by Pore-Growth Moderators. *Adv. Funct. Mater.* **2009**, *19*, 3972–3979. [[CrossRef](#)]
41. Yue, M.B.; Sun, L.B.; Zhuang, T.T.; Dong, X.; Chun, Y.; Zhu, J.H. Directly transforming as-synthesized MCM-41 to mesoporous MFI zeolite. *J. Mater. Chem.* **2008**, *18*, 2044–2050. [[CrossRef](#)]
42. Jacobs, P.A.; Beyer, H.K.; Valyon, J. Properties of the end members in the Pentasil-family of zeolites: Characterization as adsorbents. *Zeolites* **1981**, *1*, 161–168. [[CrossRef](#)]
43. Jansen, J.C.; van der Gaag, F.J.; van Bekkum, H. Identification of ZSM-type and other 5-ring containing zeolites by i.r. spectroscopy. *Zeolites* **1984**, *4*, 369–372.
44. Fang, Y.; Hu, H. An ordered mesoporous aluminosilicate with completely crystalline zeolite wall structure. *J. Am. Chem. Soc.* **2006**, *128*, 10636–10637. [[CrossRef](#)]
45. Feng, R.; Yan, X.; Hu, X.; Zhang, Y.; Wu, J.; Yan, Z. Phosphorus-modified b-axis oriented hierarchical ZSM-5 zeolites for enhancing catalytic performance in a methanol to propylene reaction. *Appl. Catal. A Gen.* **2020**, *594*, 117464. [[CrossRef](#)]
46. Battisha, I.K.; Beyally, A.E.; Mongy, S.; Nahrawi, A.M. Development of the FTIR properties of nano-structure silica gel doped with different rare earth elements, prepared by sol-gel route. *J. Sol-Gel Sci. Technol.* **2007**, *41*, 129–137. [[CrossRef](#)]
47. Göhlich, M.; Reschetilowski, W.; Paasch, S. Spectroscopic Study of Phosphorus Modified H-ZSM-5. *Microporous Mesoporous Mater.* **2011**, *142*, 178–183. [[CrossRef](#)]

Disclaimer/Publisher’s Note: The statements, opinions and data contained in all publications are solely those of the individual author(s) and contributor(s) and not of MDPI and/or the editor(s). MDPI and/or the editor(s) disclaim responsibility for any injury to people or property resulting from any ideas, methods, instructions or products referred to in the content.